FJORD ROCK SLOPE FAILURES AND TSUNAMIS

Dave van Zeyl, Department of Earth Sciences – Simon Fraser University, Burnaby, British Columbia, Canada
Doug Stead, Department of Earth Sciences – Simon Fraser University, Burnaby, British Columbia, Canada
Brian Bornhold, Coastal and Ocean Resources Inc, Sidney, British Columbia, Canada

ABSTRACT
Tsunamis can increase the existing hazard due to rock slope failures in fjord regions. Geotechnical data on potential rock slope failures are needed for prediction of tsunami run-up heights. The literature on rock slope failures in the fjords and lakes of Norway is extensive. Two potential and two past Norwegian rock slope failures have been studied in particular detail, the main features of which are summarized here. The controls on rock slope failures in fjords are discussed. The abundance of rock slope failures in Norwegian fjords could suggest that similar events have occurred in Canada but because of the relatively short documented history, the level of existing hazard from these events is largely unknown. Preliminary data on a late 16th Century rock slope failure from Knight Inlet British Columbia are provided.

RÉSUMÉ
Les tsunamis peuvent propager dans un fjord le danger lié à un éboulement au-delà de l'instabilité. Pour prédire la hauteur qu'un tel tsunami peut atteindre, il est nécessaire d'avoir des données géotechniques sur l'éboulement potentiel. La littérature historique et géologique sur les instabilités rocheuses dans les fjords et lacs en Norvège est abondante. Deux éboulements historiques ainsi que deux instabilités potentielles y ont été étudiées en particulier. Leurs principales caractéristiques sont présentées dans cet article. Le contrôle des pentes rocheuses dans les fjords norvégiens sera un objet de discussion. Leur nombre important laisse penser que des événements similaires se sont produits au Canada, cependant, étant donné le manque de documentation, le danger lié à ces instabilités n'est pas connu. Des données préliminaires sur une instabilité datant du 16th siècle dans le Knight Inlet, en Colombie Britannique, seront présentées.

1. INTRODUCTION

Rock slope failure induced tsunamis in fjords are a hazard that may often be overlooked. Rock engineers can estimate the geotechnical parameters of potential rock slope failures that are responsible for tsunami initiation and develop an understanding of the controls on rock slope stability. This paper reviews literature on rock slope failures in Norway and the controls on rock slope stability in a fjord setting. Preliminary data are presented on a rock slope failure in Knight Inlet, which is associated with a tsunami that destroyed a First Nations village in the late 16th Century.

2. TSUNAMI INITIATION

Estimation of wave run-up heights from a potential slope failure can provide planners with important information on existing hazards. Equation 1 illustrates some required geotechnical parameters for predicting initial wave height η_o after impact from a rockfall volume V with maximum height H above the water (LeBlond and Mysak 1978)

$$\eta_o^2 \approx \frac{\delta}{2\pi}\left(\frac{g'}{g}\right)\left(\frac{\rho_r}{\rho_w}\right)\left(\frac{1}{r_2^2 - r_1^2}\right)V \cdot H \qquad [1]$$

where ρ_r and ρ_w are the densities of failed rock mass and water respectively, g is the acceleration due to gravity, g' = $g(\sin\alpha - \mu\cos\alpha)$ is the effective acceleration due to gravity, α is the initial rock face slope angle and μ is the coefficient of friction; r_1 is the radial distance from the original rock face to the shoreline of the rock pile and r_2 is the radial distance to the leading edge of the wave. The fractional energy coefficient δ determines the fraction of rockfall kinetic energy that is converted to tsunami wave energy.

The variables in Equation 1 that represent or depend on geotechnical or geometric properties of the rockfall are ρ_r, α, μ, V, H, and δ. The initial rock face angle for many rockfalls is in the range 70-90°, thus facilitating the assumption that g' and g are nearly equal. The rockfall volume, maximum height, and fractional energy coefficient are relatively difficult parameters to predict, rockfall volume being a particularly effective predictor of wave height (Murty 2003). It is commonly assumed that only a small fraction of the kinetic energy of the failed material, e.g. 1% (Murty 1979), is converted to tsunami wave energy. The rock engineer must devise a means for estimating the relevant geotechnical parameters in the prediction of the initial tsunami wave character.

3. NORWEGIAN ROCK SLOPE FAILURES

In Norway the history of rock slope failures into fjords and lakes is well documented (e.g., Bjerrum and Jørstad 1968; Grimstad and Nesdal 1991; Furseth 1995) dating as far back as 700 years (Furseth in press). Many lives have been claimed in the events, including more than 255 since

the start of the 16th Century (Table 1). The Geological Survey of Norway (NGU) in consultation with Astor Furseth has assembled a database containing over 3000 landslide and snow-avalanche events. Table 1 summarizes selected properties of 29 historical rock avalanche (fjellskred) events in western Norway for which there are volume estimations. These volumes span three orders of magnitude and initiate from maximum release heights of 200-1200 m above sea level. Over 75% of these events initiated in dioritic to granitic gneiss. These data provide an indication of typical values for the geotechnical parameters in Equation 1.

Table 1 Selected historic Norwegian rock avalanches

Characteristic	Value[1]
Min volume (10^6 m^3)	0.01
Max volume (10^6 m^3)	12
Min release height (m)	200
Max release height (m)	1200
Max wave height (m)	74
Total lives lost	255

[1]Data retrieved from NGU database: www.skrednett.no

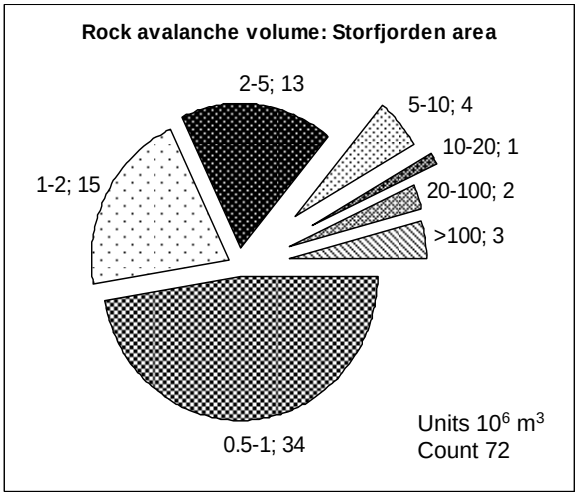

Figure 1 Rock avalanche volumes (Blikra et al. 2005)

Since the 1990s the NGU and the NGI (Norwegian Geotechnical Institute), under the auspices of the ICG (International Centre for Geohazards) have undertaken extensive studies of rock avalanches and rock-slope failures onshore and in the fjords of Norway. The magnitude (e.g., Fig. 1) and spatial pattern of rock avalanche deposits beneath the fjords have been established by swath bathymetric surveys (Blikra et al. 2002). Figure 1 shows the volume distribution of rock-avalanche deposits in the Storfjorden area. Five of these events are larger (>12 x 10^6 m^3) than the historical events that are referred to in Table 1, the largest being 400 M m^3. However, the vast majority (68%) have magnitudes that are less than 2 M m^3.

In west Norway rock avalanches are concentrated in the inner fjords, with fewer rock avalanches found onshore (Blikra et al. 2006). A number of sediment cores (Lepland et al. 2002) and seismic stratigraphy have been used to establish the past frequency of rock avalanches. These events are concentrated within the second half of the Holocene in the inner fjord areas of west Norway (Blikra et al. 2006). These data have been used to make preliminary hazard assessments, which have revealed annual probabilities of occurrence greater than 10^{-6} for large rock avalanche events ($V \geq 1$ M m^3) in parts of the Storfjorden area (Blikra et al. 2005).

Rock engineering studies (e.g., Bhasin and Kaynia 2004) have been carried out on primarily four rock slope failures in west Norway (Fig. 2): Oppstadhornet, Åknes, Tafjord, and Loen. Results from these site investigations allow for a consideration of the controls on the underlying mechanics of the rock slope failures.

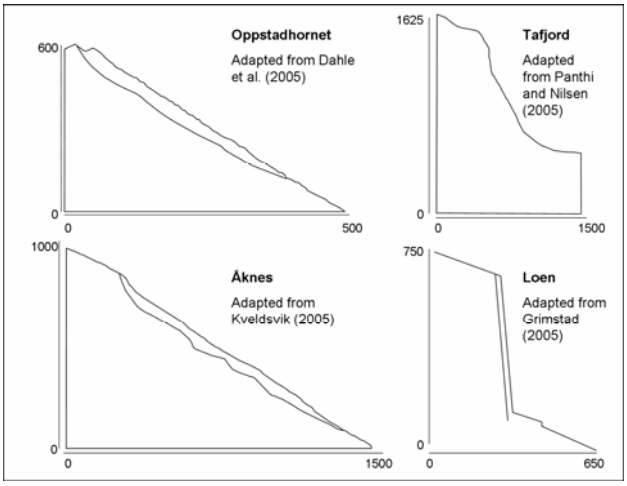

Figure 2 Approximate rock slope profiles

3.1 Rock slope characteristics

3.1.1 Oppstadhornet

Oppstadhornet is a 700-m high potential multiple block wedge and/or sliding failure in a uniformly 40° dipping southeast facing slope composed of various well foliated very strong gneissic rocks particularly tonalite and amphibolitic gneiss (Bhasin and Kaynia 2004; Dahle et al. 2005). The rock mass at Oppstadhornet is good to very good quality with an average *Q*-value of 40 (Bhasin and Kaynia 2004). The base of the wedge complex is defined by a 40-70° southeast dipping rear shear plane developed along the foliation and a 60° southwest dipping eastern shear plane. Kinematic freedom is provided by a 185° trending 36° plunging wedge intersection daylighting in the 40° slope face. This freedom is restricted since the

southwest margin of the wedge complex is in contact with a reactivated subvertical northeast dipping fault (Dahle et al. 2005) and the trend of the wedge intersection is oriented at 45° to the strike of the slope. The overall block mass movement direction has been to the southeast thus facilitated largely by the rear shear plane and this is also indicated by a 20 to 40-m high southeast facing down-slope dipping back scarp (Bhasin and Kaynia 2004). This global movement includes a backwards rotational component (Blikra et al. 2002), which has placed the wedge complex over a more shallowly dipping portion of the rear shear plane thus reducing the driving force (Dahle et al. 2005).

Numerical modelling investigations at Oppstadhornet have revealed that the entire volume of the potentially unstable mass is 20 M m^3 although the magnitude depends on the driving and resisting forces involved (Bhasin et al. 2004). The unstable volume may be in the order of 5-7 M m^3 if the residual friction angle of the basal surface is reduced to 25° or if the slide mass is subjected to a dynamic excitation equivalent to an earthquake with a 475-year return period (Bhasin and Kaynia 2004). Water pressures of more than 0.1 MPa are also capable of initiating instability within the slide mass (Dahle et al. 2005).

3.1.2 Åknes

Åknes is a potential 1000-m high multiple block sliding failure in a south-southeast (153-160°) facing 34-40° dipping inner fjord slope in granitic, dioritic and biotitic gneiss (Kveldsvik et al. 2006). The granitic gneiss varies from massive to densely jointed while the dioritic gneiss is consistently massive and the biotitic gneiss comprises densely foliated weak layers. Typical block size is between 0.1 and 3 m^3 (Lied and Kristensen 1996). The strength of the intact rock ranges from strong to very strong depending partly on the concentration of biotite. Uniaxial compressive strengths range from 85 to 330 MPa (Kveldsvik 2005). An upper 700-m long tension crack extending between 650 and 1000 m a.s.l. exhibits a 20-30 m opening along the upper western segment and tapers to about 1 m along the lower eastern portion (Kveldsvik et al. 2006). Smaller cracks that are subparallel to the uppermost crack exist throughout the height of the slope and seem to cut the unstable mass into separate blocks (Kveldsvik 2005).

Three discontinuity sets have been identified at Åknes. A joint set is developed along the foliation, whose global mean vector (GMV) from 143 field measurements dips 23° to the south-southeast (155°) but whose orientation is spatially variable throughout the unstable mass (Kveldsvik et al. 2006). Foliation joints surrounding the upper crack have a mean dip of 20° to the east (076°) while in the middle and lower areas these joints dip 30° to the south (180°), which is subparallel to the slope (Kveldsvik et al. 2006). Derron et al. (2005) also measured the mean orientation of the foliation joints (J1) in the upper part of the slope (Fig. 3). Kinematic feasibility exists for sliding along the foliation joints. The two other sets (J2 and J3) provide potential lateral release surfaces for a slide mass (Fig. 3). Comparing the joint orientation data and the average surface movement direction (Fig. 3) sliding along the intersection between the foliation and the northeast dipping joint set is both kinematically feasible and an active mode.

Four boreholes on Åknes reveal that the incidence of joints decreases consistently with depth, below 60 m few discontinuities are found, and zones of crushed rock are found at various levels that are confined to the upper 60 m depth (Kveldsvik et al. 2006). These data indicate that potential rupture surfaces and the presence of secondary permeability are confined within the upper 60 m depth. Further to this, data from a 2D resistivity survey suggests that the 1350 m long rupture surface consists of about five concave upwards undulations reaching maximum depths of about 60 m (Kveldsvik 2005). Preliminary numerical modelling indicates that global movement along the serrated rupture surface is best achieved when the slide mass is more heavily jointed resulting in increased kinematic freedom, or when pore pressures are introduced (Kveldsvik 2005).

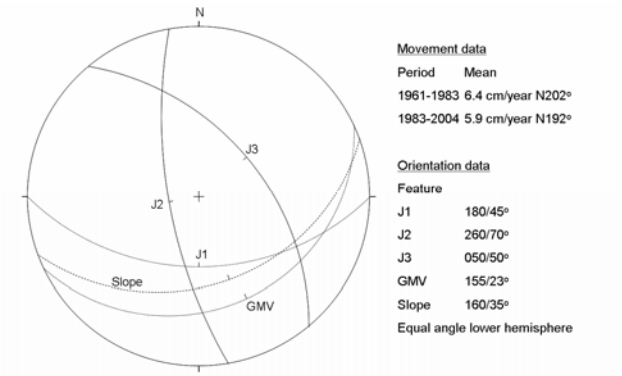

Figure 3 Kinematic summary for Åknes

3.1.3 Tafjord

Furseth (1985) describes in detail the 1.5 M m^3 rockfall and resulting 62-m high tsunami in the innermost branch of Norddalsfjord that occurred on 7 April 1934 killing 41 people. The blocky rock material fell from a maximum height of 730 m in the 800-900 m southwest facing 60° slope (Bjerrum and Jørstad 1968) at Langhammaren. The 1934 Tafjord event initiated predominantly as a sliding failure defined by rupture along foliation in mica gneiss dipping 60° to the south, although the intersection between this surface and a structure dipping 80° approximately to the west (Waltham 2002) comes very close to daylighting in the slope surface. This suggests that a certain amount of sliding occurred along the subvertical structure. The rupture surface along the foliation could have developed following biotite-rich layers in the mica gneiss (Hermanns et al. 2006). The mica gneiss has moderate strength overall with measured uniaxial compressive strength of 67 MPa (Panthi and Nilsen 2005).

Numerical analysis of the stresses at this site has indicated a particularly high (up to 110) ratio of major to minor stress 40 m beneath the slope surface under a convex portion of the slope profile near the crest (Panthi and Nilsen 2005). This state of stress likely developed after the 1934 slide mass was released. Broch and Sørheim (1984) indicate that highly anisotropic stress conditions are common near fjord slopes that exhibit extreme topography. As an example, rock stress induced stability problems are common in the walls of tunnels nearest to large and steep fjord slopes and are uncommon on the opposite tunnel walls.

3.1.4 Loen

The Ramnefjell is a 1000-1200 m high east facing slope at Loen Lake, which has been the site of seven rock slides between 1905 and 1950 totalling more than 4 M m^3 of transported material and each resulting in flood waves two of which took 134 lives in total (Grimstad 2005). The lower part of the slope dips at about 65^o while the upper portion is nearly vertical (Bjerrum and Jørstad 1968). The rock type is very strong gneiss with weaker zones of amphibolite and chlorite schist.

Three rough and undulating discontinuity sets have been identified at Loen, and are described by Grimstad (2005). A regional-scale mode 1 fracture set parallels the upper portion of the slide scar at Ramnefjell dipping 80^o to the east. The spacing and persistence of this set are inversely related to scale. Extremely widely spaced joints of this set are continuous *en-echelon* for the height of the slide scar while at a finer scale the joints are discontinuous and spacing is between 0.5 and 2 m. A set of widely spaced joints is established along the foliation dipping 35-40^o to the east-southeast in the north and 22-36^o to the south in the south part of Ramnefjell. A third set comprises subvertical extremely widely spaced and sometimes very highly persistent joints that are approximately orthogonal to the slope. These data indicate kinematic feasibility for sliding along the foliation in the north part of the slope with the first set providing tensile release and the third set providing lateral release.

Grimstad (2005) calculated the stresses for the 7-m thick column at the base of the 1905 failure and made two independent estimates of the shear strength along the foliation surface. He found that in the dry state the past failure could not have initiated. Additional driving force was needed, such as water pressures along the subvertical joint, and/or a reduction in shear resistance was required, likely caused by uplift from water pressures along the foliation resulting in reduced effective normal stresses.

3.2 Controls

Based on the extensive literature available on rock slope failures in Norway and supplemented by additional rock slope engineering literature the following represent the dominant controls on rock slope stability in fjord settings involving strong jointed rock masses.

3.2.1 Kinematics and state of stress

A global failure surface in a rock mass comprised of strong intact rock strength is more likely to follow existing discontinuities (e.g., master joints, faults, or foliation) than to emerge following new intact rock fractures. The first and foremost prerequisite for failure therefore is kinematic admissibility.

Primary kinematic freedom is often derived from discontinuities established along the foliation, which results from endogenic processes (e.g., regional crustal compression). Exfoliation surfaces frequently provide lateral and/or tensile release surfaces (e.g., Loen). Exfoliation surfaces form because of a specific state of stress within the slope that is associated with relatively recent excavation into the fjord-slope by exogenic processes (e.g., glacial, colluvial).

3.2.2 Rock mass strength

The degree of jointing, intact rock strength and its variability, and the shear strength of discontinuities are important properties of a rock mass (Edelbro 2003). The foliation surfaces that often form basal sliding surfaces are commonly serrated because of variability in the dip angle of foliation. The ability of a slide mass to translate over a serrated surface is directly related to the degree of jointing within the rock mass (Corkum and Martin 2004; Kveldsvik 2005). The scale of rock slopes in fjords coupled with a high degree of jointing can lead to rupture surfaces that step from one structure to another resulting in a surface that is more complex than one that follows a single persistent structure (Sjöberg 1999). The gneissic rocks associated with many of the slope failures in west Norway host zones of weaker material such as amphibolite. These weak zones are host to a relatively high incidence of discontinuities, will yield more often in the presence of an adverse state of stress, and readily provide a place for discontinuities of low strength to develop. Finally, the shear strength of discontinuities will play a major role (Bhasin et al. 2004; Dahle et al. 2005) in controlling block movement.

3.2.3 Water pressure

Water pressure can reduce stability in two ways. The shearing resistance along a slide surface is reduced when the effective normal stress is lowered in the presence of water pressures. Water can act as a driving force when a release surface contains a significant water column (e.g. Loen). Terzaghi (1962) referred to the cold and wet period between 1720 and 1760 when the frequency of rockslides was exceptionally high to emphasize the importance of cleft-water pressures. Similarly, Bjerrum and Jørstad (1968) noted spring and fall maxima in the seasonal frequency of small rockfalls.

3.2.4 Earthquakes

Earthquakes, like water pressures, are both *triggers* of slope failures and *causes* of progressive failure. Spatial correlations based on empirical relationships between earthquake magnitude and aerial extent of affected region (Keefer 1984) are observed for clusters of rock avalanches in the inner fjord areas of west Norway clustering near a post *Younger Dryas* (<11 500 BP) fault (Blikra et al. 2002). Parametric studies (Bhasin et al. 2004) illustrate that ground accelerations are capable mechanically of inducing fjord rock slope failures.

3.2.5 Time

More than 10,000 years have passed since the fjords were filled with glacier ice. Near-surface thermal (Watson et al. 1999), hydrological (Stewart and Ripley 1999) and freeze-thaw cycles operating at a variety of time-scales surely have played a role in the development of unstable rock slopes. The fact that there is a concentration of rock avalanche events clustered in the second half of the Holocene in the inner fjord areas of Norway (Blikra et al. 2006) suggests that a certain amount of time was required for the rock slopes to fail.

4. KNIGHT INLET

Native oral historical, archaeological and geological evidence suggests that the First Nations village of Kwalate in Knight Inlet British Columbia was destroyed by a rock slope failure induced tsunami in the late 1500s (McLaren et al. 2005). No temporal correlation between the tsunami and a corresponding rockfall exists; however, three large rock slopes exist across the fjord from the Kwalate village (Fig. 4). Anecdotal evidence (e.g., Proctor and Maximchuk 2003: 188) suggests that a rockfall at Adeane Point (Fig. 5), here termed the *Adeane rock slope*, was responsible for the disaster. This rock slope has a relatively active appearance, and swath bathymetric data have revealed an estimated 4 M m^3 conical debris pile extending 800 m from the base of the slope (Fig. 4 inset). Preliminary data are presented below on the geology and geomorphology of Knight Inlet, and on the Adeane rock slope and debris pile.

4.1 Geology and geomorphology

Along the southeast shore of Knight Inlet from Duncan Point to Millerd Creek (Fig. 4) the shoreline aligns to 036^o and the fjord is up to 542 m deep in this area. The slopes rise to between 800 and 1600 m a.s.l. and are underlain mainly by late Jurassic to early Tertiary tonalitic, quartz dioritic and dioritic rocks (Roddick and Woodsworth 2006). A local pendant comprised of Upper Triassic basalt interbedded with minor crystalline limestone and biotite-chlorite schist outcrops in the 880 m 55^o Adeane rock slope (Roddick, 1977). The mean orientation of the northeast contact of this pendant between Loughborough and Knight Inlet is 311^o and this orientation represents approximately that of many other geological units in the region (Roddick and Woodsworth 2006). These data suggest that this segment of Knight Inlet can be classified as a concordant transverse reach since it cuts northeast across the geological grain by nearly a right angle (Peacock, 1935).

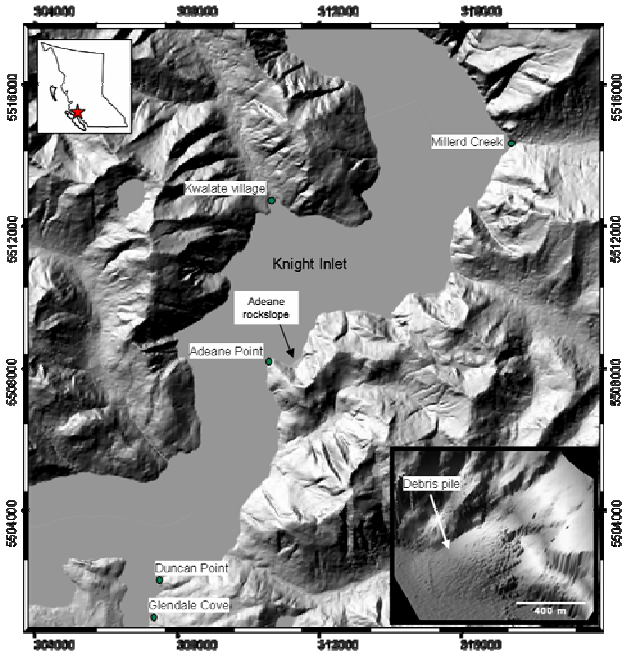

Figure 4 Study site in Knight Inlet British Columbia

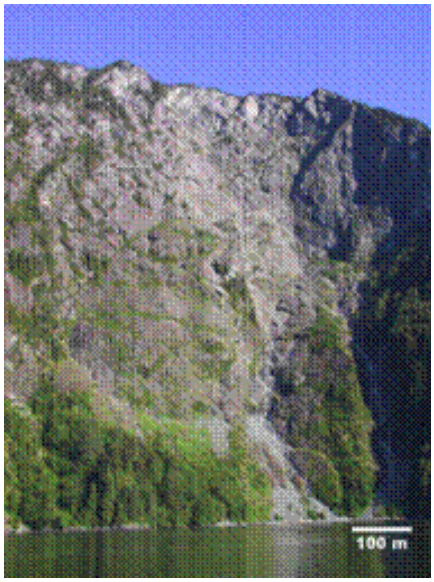

Figure 5 Adeane rock slope (B. Bornhold)

Little to no structural data exist for the Adeane rock slope. The dominant structure in the pendants in this region is

foliation dipping steeply to the northeast (Woodsworth et al. 1991). Dura and Rusmore (2003) mapped 251 brittle Miocene faults in Knight Inlet then divided the dataset into NW-SE and NE-SW striking populations. The majority of these faults were small-scale and steep with strike-slip motion indicated although 19 of the faults were shallow. Bancroft (1913: 110) described the regional presence of two sets of joints trending NW-SE and NE-SW that are either vertical or dip steeply to the northeast; and he believed that regional sets of faults paralleled the two sets of joints. Peacock (1935: 684) suggested that the NW-SE set of fractures represent tensile fractures having relatively large apertures and the NE-SW set of fractures are shear fractures that tend to be closed. This suggestion is supported by data from Schofield (1925). These data suggest that steeply northeast and northwest dipping structures are likely present at the Adeane rock slope.

Recent helium isotopic data from the Klinaklini River valley at the head of Knight Inlet (Shuster et al. 2005) suggest a period of rapid denudation of 1700 to 2200 m beginning at 1.8 Ma and ensuing through 1.4 Ma. These data may suggest that Knight Inlet was excavated chiefly by glacial erosion during the period 1.8 through 1.4 Ma.

4.2 Adeane debris pile

Block size was assessed from 59 bathyscopic photos (e.g., Fig. 6) taken from a submersible during an exploration beneath the Adeane rock slope in spring 2005. The diameter of the equivalent sphere was calculated using the program WipFrag (WipWare 2002) after manually delineating block edges for between 3 and 15 blocks in each photo. The average of the mean block size computed from each of the 59 photos is 0.4 m. The smallest block size measured was 0.05 m although smaller blocks can be seen in some of the photographs. The maximum dimension of the field of view in the photographs is about 1.8 m and blocks larger than this exist. Some degree of comminution during transport would make the block size in the debris pile less than the *in situ* block size in the source area. With respect to block size in the source-area, the minimum is therefore greater than 0.05 m the mean is greater than 0.4 m and the maximum is greater than 1.8 m. These preliminary data suggest that the rock mass in the source area is predominantly very blocky to blocky (Cai et al. 2004).

4.3 Adeane rock slope

A pre-field structural geology assessment from air photographs has been used in conjunction with knowledge of the regional geology to perform a preliminary kinematic analysis for the Adeane rock slope.

A sharp contact exists at the Adeane rock slope between the greenstone pendant and strongly foliated diorite (Roddick 1977). Foliation at the base is dipping 52^{o} to 012^{o} (Roddick and Woodsworth, 2006). Few other data can be found in the literature on the structural geology at this site. An engineering geological site characterization will be undertaken in summer 2006 to complement and verify the preliminary interpretations described below.

Aspect along the slope crest was measured from a 1:15,000-scale aerial photo using a continuous sequence of 30 m lines. A circular histogram of the measurements is shown in Figure 7. On average, the crest of the slope faces 332^{o}. The part of the crest that is underlain by greenstone (Roddick and Woodsworth, 2006) faces consistently to the north (009^{o}). Where the crest is underlain by diorite (Roddick and Woodsworth, 2006) the slope faces on average to the west-northwest (291^{o}). A relatively short segment of the crest located at the contact between the greenstone and the diorite is facing to the northwest (327^{o}). The slope is dipping 55^{o} overall although many portions appear to be subvertical.

Figure 6 Bathyscopic photograph of blocks (B. Bornhold)

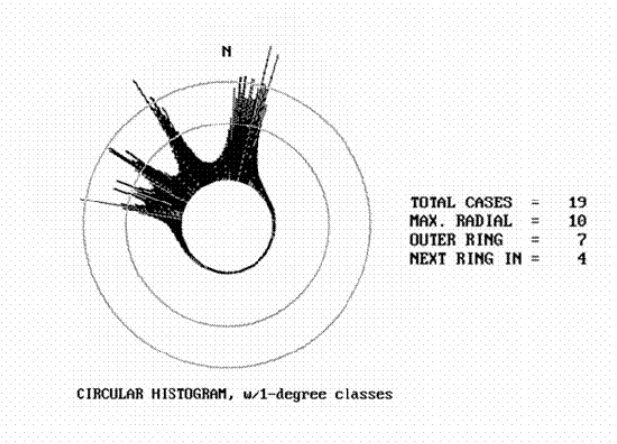

Figure 7 Aspect at slope crest of Adeane rock slope

From these data the west part of the crest appears to reflect foliation (S1) in the greenstone, and the east part may emerge as a steeply west-northwest dipping structure (S2) in the diorite. The central portion of the crest may represent the intersection between these first two

structures. A stereonet combining the dip directions of the two structures and the average aspect of the crest with the common overall inclination of the slope (55^{o}) was examined. This suggests that the two structural sets intersect and form wedges that daylight the slope face. Field data is needed to confirm the orientation of these structural sets and on their spacing and persistence in order to reveal the geometry of past and potential failures.

The program SWEDGE (Rocscience, 2005) was used to perform a Monte Carlo simulation on the preliminary interpreted geometry of the Adeane rock slope as described above. The dip and dip direction of the two structures (assuming single fully-persistent structures) and the overall slope were assumed as random normal variables with standard deviation 2^{o} and the height of the slope was assigned as 880 m. The average wedge volume from this simulation, which assumes that the failure volume comprises one large wedge, was 1.3 M m^3 (Fig. 8) although the possible volume can exceed 4 M m^3. Because of the preliminary nature of these data, no conclusions can be drawn until a full engineering geological assessment has taken place.

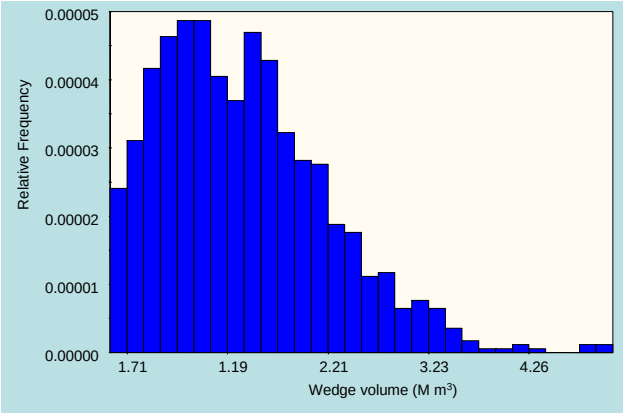

Figure 8 Distribution of wedge failure volume based on a preliminary structural geology assessment

5. CONCLUSION

This paper has reviewed rock slope failures associated with tsunamis in Norway and a similar event in British Columbia. The preliminary investigation indicates that further work is required to investigate the hazard from these events in western North America.

6. ACKNOWLEDGEMENTS

Astor Furseth translated Norwegian field names from the NGU national database of avalanches and landslides. R. Bhasin, L.H. Blikra, H. Dahle, and V. Kveldsvik provided copies of relevant papers and provided helpful comments on parts of this paper. Funding provided by an NSERC Discovery grant to second author.

References

Bancroft, J.A. 1913. Geology of the coast and islands between the Strait of Georgia and Queen Charlotte Sound, B.C., *Geological Survey of Canada, Memoir* 23, p. 152

Bhasin, R. and Kaynia, A.M. 2004. Static and dynamic simulation of a 700-m high rock slope failure in western Norway. *Engineering Geology*, 71: 213 – 226

Bhasin, R., Kaynia, A. Blikra, L.H., Braathen, A. and Anda, E. 2004. Insights into the deformation mechanisms of a jointed rock slope subjected to dynamic loading, Paper 2B 21 – SINOROCK2004 Symposium, *International Journal of Rock Mechanics & Mining Sciences*, 41(3): p. 6

Bjerrum, L. and Jørstad, F. 1968. Stability of rock slopes in Norway, *Norwegian Geotechnical Institute Publication* 79: 1 - 11

Blikra, L.H., Braathen, A., Anda, E., Stalsberg, K. and Longva, O. 2002. Rock avalanches, gravitational bedrock fractures and neotectonic faults onshore northern West Norway: Examples, regional distribution and triggering mechanisms, *Geological Survey of Norway Report 2002.016*, Trondheim, p. 53

Blikra, L.H., Longva, O., Harbitz, C. and Lovhølt, F. 2005. Quantification of rock-avalanche and tsunami hazard in Storfjorden, western Norway, *Landslides and Avalanches, ICFL 2005*, Trondheim, Norway, pp. 57 – 63

Blikra, L.H., Longva, O., Braathen, A., Anda, E., Dehls, J.F. and Stalsberg, F. 2006. Rock slope failures in Norwegian fjord areas: Examples, spatial distribution, and temporal pattern, *In* Evans, S.G. Scarawcia Mugnozza, G., Strom, A.L. and Hermanns, R.L. (eds.), *Massive rock slope failure: new models for hazard assessment*, Kluwer, Dordrecht, Netherlands.

Broch, E. and Sørheim, S. 1984. Experiences from the planning, construction and supporting of a road tunnel subjected to heavy rockbursting, *Rock Mechanics and Rock Engineering*, 17: 15 - 35

Cai, M., Kaiser, P.K., Uno, H., Tasaka, Y. and Minami, M. 2004. Estimation of rock mass deformation modulus and strength of jointed hard rock masses using GSI, *International Journal of Rock Mechanics & Mining Sciences*, 41(1): 3 - 19

Corkum, A.G. and Martin, C.D. 2004. Analysis of a rock slide stabilized with a toe-berm: a case study in British Columbia, Canada, *International Journal of Rock Mechanics & Mining Sciences*, 41: 1109 - 1121

Dahle, H., Nilsen, B., Blikra, L.H. and Braathen, A. 2005. Numerical study of stability for Oppstadhornet rock-slope failure, *Landslides and Avalanches, ICFL 2005*, Trondheim, Norway, pp. 83 - 88

Derron, M.-H., Blikra, L.H. and Jaboyedoff, M. 2005. High resolution digital elevation model analysis for landslide hazard assessment (Åkerneset, Norway), *Landslides and Avalanches, ICFL 2005*, Trondheim, Norway, pp. 101 - 106

Dura, T. and Rusmore, M. 2003. Cenozoic faulting in Knight Inlet, *Southern California Conference on Undergraduate Research*, 22 November 2003, University of California, Irvine, California, USA

Edelbro, C. 2003. Rock mass strength: A review, *Technical Report* 2003:16, Department of Civil Engineering, Division of Rock Mechanics, Luleå University of Technology, Luleå, Sweden, p. 160

Furseth, A. 1985. *Dommedagsfjellet – Tafjord 1934*, Gyldendal Norsk Forlag A/S, Oslo, Norway, p. 104 (in Norwegian with English summary)

Furseth, A. in press. *Avalanche disasters in Norway* (in Norwegian with English summary)

Grimstad, E. and Nesdal, S. 1991. The Loen rockslides. A historical review. *Norges Geotekniske Institutt Publikasjon*, 182: 1 - 6.

Grimstad, E. 2005. The Loen rock slide – an analysis of the stability, *Landslides and Avalanches, ICFL 2005*, Trondheim, Norway, pp. 129 - 135

Hermanns, R.L., Blikra, L.H., Naumann, M., Nilsen, B., Panthi, K.K., Stromeyer, D. and Longva, O. 2006. Examples of multiple rock-slope collapses from Köfels (Ötz valley, Austria) and western Norway, *Engineering Geology*, 83: 94 - 108

Keefer, D. 1984. Landslides caused by earthquakes, *Geological Society of America Bulletin*, 95: 406 - 421

Kveldsvik, K. 2005. Numerical modelling for rock engineering. Assignment from Vidar Kveldsvik: Numerical modelling of the Åkerneset landslide by use of UDEC, *Norwegian Geotechnical Institute* GB 8304, Oslo, p. 15

Kveldsvik, K., Eiken, T., Ganerød, G.V., Grøneng, G. and Ragvin, N. 2006. Evaluation of movement data and ground conditions for the Åknes rock slide, *International Symposium on Stability of Rock Slopes in Open Pit Mining and Civil Engineering Situations, The South African Institute of Mining and Metallurgy*, Cape Town, South Africa, Series S44: pp. 279 - 299

LeBlond, P.H. and Mysak, L.A. 1978. *Waves in the Ocean*, Elsevier, Amsterdam, Netherlands, p. 602

Lepland, A., Bøe, R., Sønstegaard, E., Haflidason, H., Hovland, C., Olsen, H. and Sandnes, R. 2002. Sedimentological descriptions and results of sediment cores from fjords and lakes in northwestern Norway – final report, *Geological Survey of Norway Report 2002.014*, Trondheim, p. 49

Lied, K. and Kristensen, K. 1996. Åkernes landslide. General description of the Åkernes slide area and control measures, *Norwegian Geotechnical Institute Report* 585910-9, Oslo, p. 11

McLaren, D., Bornhold, B.D., and Harper, J. 2005. Archaeological and oral historical evidence of an ancient tsunami event at Kwalate, Knight Inlet, Report submitted to the Da'naxda'xw First Nation and B.C. Archaeology Branch, January 2005, p. 46

Murty, T.S. 1979. Submarine slide-generated water waves in Kitimat Inlet, British Columbia, *Journal of Geophysical Research*, 84 (C12): 7777 – 7780

Murty, T.S. 2003. Tsunami wave height dependence on landslide volume. *Pure and Applied Geophysics*, 160: 2147 – 2153

Panthi, K.K. and Nilsen, B. 2005. Numerical analysis of stresses and displacements for the Tafjord slide, Norway. *Bulletin of Engineering Geology and the Environment*, DOI 10.1007/s10064-005-0009-y

Peacock, M.A. 1935. Fjord-land of British Columbia. *Bulletin of the Geological Society of America*, 46: 633 – 696

Proctor, B. and Maximchuk, Y. 2003. *Full Moon Flood Tide: Bill Proctor's Raincoast*, Harbour, Madeira Park, British Columbia, Canada, p. 288

Rocscience 2005. SWEDGE, Version 4.080, Rocscience Inc, Toronto, Ontario, Canada

Roddick, J.A. 1977. Notes on the stratified rocks of Bute Inlet Map-Area (excluding Vancouver and Quadra Islands), *Geological Survey of Canada Open File,* 480: p. 20

Roddick, J.A. and Woodsworth, G.J. 2006. Geology, Bute Inlet, British Columbia, *Geological Survey of Canada, Open File* 5037: scale 1: 250,000

Schofield, S.J. 1925. The fissure systems of British Columbia, *Canadian Institute of Mining and Metallurgy Bulletin,* 159: 759 - 764

Sjöberg, J. 1999. Analysis of large scale rock slopes, *Doctoral Thesis* 1999:01, Division of Rock Mechanics, Luleå University of Technology, Luleå, Sweden, p. 788

Shuster, D.L., Ehlers, T.A., Rusmore, M.E. and Farley, K.A. 2005. Rapid glacial erosion at 1.8 Ma revealed by $^{4}He/^{3}He$ thermochronometry, *Science*, 310: 1668 - 1670

Stewart, T. and Ripley, B.D. 1999. Deformation analysis of the Wahleach rock slope, southwest British Columbia, *In* Detournay, C. and Hart, R. (eds), *FLAC and Numerical Modelling in Geomechanics*, Proceedings of the Conference, Minneapolis, September 1999, Balkema, Rotterdam, pp. 55 - 62

Terzaghi, K. 1962. Stability of steep slopes on hard unweathered rock, *Géotechnique*, 12(4): 251 – 270

Waltham, T. 2002. Unloading joints and rockfalls in Norway's fjordlands, *Geology Toda*y, 18(6): 220 – 225

Watson, A.D., Moore, R.D. and Stewart, T.W. 2004. Temperature influence on rock slope movements at Checkerboard Creek, *In Proceedings of the 9th International Symposium on Landslides: Evaluation and Stabilization*, Rio de Janeiro, Brazil, 28 June – 2 July 2004, pp. 1293 – 1298

WipWare 2002. WipFrag, Version 2.2, WipWare Inc, Bonfield, Ontario, Canada

Woodsworth, G.J., Monger, J.W.H., and Gabrielse, H. 1991. *Part B. Coast Belt* [Chapter 17 Structural Styles], In Gabrielse, H. and Yorath, C.J. (eds), Geology of the Cordilleran Orogen in Canada, Geological Survey of Canada, Geology of Canada Series 4, pp. 581 - 591